ISSN 1674-1056
http://cpb.iphy.ac.cn
http://iopscience.iop.org/cpb
中国物理 B
Chinese Physics
中国物理 Chinese Physics B

Quantum steering in Heisenberg models with Dzyaloshinskii-Moriya interactions

Hui-Zhen Li(李慧贞), Rong-Sheng Han(韩榕生), Ye-Qi Zhang(张业奇), Liang Chen(陈亮)

Citation: Chin. Phys. B . 2018, 27(12): 120304. **doi:** 10.1088/1674-1056/27/12/120304
Journal homepage: http://cpb.iphy.ac.cn; http://iopscience.iop.org/cpb

What follows is a list of articles you may be interested in

Transferring information through a mixed-five-spin chain channel

Hamid Arian Zad, Hossein Movahhedian

Chin. Phys. B . 2016, 25(8): 080307. **doi:** 10.1088/1674-1056/25/8/080307

Thermal entanglement of the Ising–Heisenberg diamond chain with Dzyaloshinskii–Moriya interaction

Qiao Jie, Zhou Bin

Chin. Phys. B . 2015, 24(11): 110306. **doi:** 10.1088/1674-1056/24/11/110306

Characterizing the dynamics of quantum discord under phase damping with POVM measurements

Jiang Feng-Jian, Ye Jian-Feng, Yan Xin-Hu, Lü Hai-Jiang

Chin. Phys. B . 2015, 24(10): 100304. **doi:** 10.1088/1674-1056/24/10/100304

Quantum correlation dynamics in a two-qubit Heisenberg XYZ model with decoherence

Yang Guo-Hui, Zhang Bing-Bing, Li Lei

Chin. Phys. B . 2015, 24(6): 060302. **doi:** 10.1088/1674-1056/24/6/060302

Quantum correlations in a two-qubit anisotropic Heisenberg *XYZ* chain with uniform magnetic field

Li Lei, Yang Guo-Hui

Chin. Phys. B . 2014, 23(7): 070306. **doi:** 10.1088/1674-1056/23/7/070306

Quantum steering in Heisenberg models with Dzyaloshinskii–Moriya interactions*

Hui-Zhen Li(李慧贞), Rong-Sheng Han(韩榕生), Ye-Qi Zhang(张业奇), and Liang Chen(陈亮)†

Mathematics and Physics Department, North China Electric Power University, Beijing 102206, *China*

(Received 15 July 2018; revised manuscript received 9 September 2018; published online 10 November 2018)

In this work, we study the quantum steering in two-qubit Heisenberg models with Dzyaloshinskii–Moriya (DM) interaction and an external magnetic field. We find that the steerable weight (SW) and the critical temperature where SW $\to 0$ can be enhanced by the DM interactions. In the special case where the magnetic field is vanishing and the two spins are ferromagnetically coupled, the DM interaction can tune the zero-temperature SW from zero to a finite value. In addition to the SW, some other measurements used to identify the quantum entanglement and quantum correlations are investigated, *i.e.*, the concurrence, the quantum discord, and the robustness of coherence. In the strong magnetic field limit, our results show that the SW is dramatically different from the other measurements.

Keywords: quantum steering, Heisenberg model, Dzyaloshinskii–Moriya interaction

PACS: 03.67.–a, 03.65.Ud, 75.10.Jm, 75.10.Pq **DOI:** 10.1088/1674-1056/27/12/120304

1. Introduction

Quantum entanglement, a unique concept in quantum mechanics, refers to the special relationship between two parties in a quantum system,[1] even though these two parties are far from each other. Numerous measurements[2–7] have been proposed to describe quantum entanglement and nonlocal quantum correlations, *e.g.*, concurrence, quantum discord, and quantum coherence. Quantum steering is a typical measurement to identify quantum entanglement. This aspect can be traced back to 1935 by Schrödinger[8,9] as a generalization of the Einstein–Podolsky–Rosen paradox[10] for arbitrary pure entangled quantum states. In 2007, Wisemann *et al.* found an operational method to identify quantum steering expressed in mathematical representation.[11] Briefly, quantum steering is defined under the following scenario. Consider a bipartite quantum state shared by Alice and Bob. Bob trusts his own measurements and believes that the state can be described by a local hidden state[12] model. In order to convince Bob that the state is quantum entangled, Alice performs her own measurement using the scheme proposed by Bob temporarily and informs him of her results. If the results of Alice and Bob's measurements cannot be explained by any local hidden state theory, *i.e.*, Alice has the magic power to predict Bob's result before his measurement, Bob will believe that there does exist some quantum entanglement. Quantum steering has attracted great attention in recent years in terms of both theoretical development[13–19] and experimental investigation.[20–24] This measurement plays an important role in a broad range of quantum information, such as quantum teleportation,[25] quantum key distribution,[26] and quantum computation.[27]

2. Model Hamiltonians

In this work, we study the two-qubit Heisenberg model (generally, the XYZ model) subject to Dzyaloshinskii–Moriya (DM) interactions and an external magnetic field. Three models are investigated. The first one is the XXZ model subject to a z-component DM interaction without a magnetic field. The second one is similar to the first one, the only difference is that the z-component DM interaction has been replaced by an x-component DM interaction. The third one is the general case, the XYZ model subject to a z-component DM interaction and external magnetic field. The analytic expressions of the finite temperature density matrix for all these models can be calculated explicitly. The first model is a special case of the third one. We present it separately as the first case such that we can compare the impact of z and x components of the DM interaction on quantum correlations straightforwardly. The impacts of the DM interaction on quantum correlations in a two-qubit Heisenberg model have been investigated in previous studies,[28–30] and include thermal entanglement, concurrence, and quantum discord. However, quantum steering for the Heisenberg model with DM interaction has not been investigated as far as we know.

The first Hamiltonian is the two-qubit XXZ model with a z-component DM interaction, which is given by the following formula[31]

$$H_1 = J\left(S_1^x S_2^x + S_1^y S_2^y\right) + J_z S_1^z S_2^z + D_z(S_1^x S_2^y - S_1^y S_2^x), \qquad (1)$$

where J and J_z are the Heisenberg coupling constants between the two spins, D_z is the z-component parameter of the DM interaction, and S_j^x, S_j^y, and S_j^z are the three spin-operators located at the j-th site ($j = 1, 2$). Their explicit expressions for

*Project supported by the National Natural Science Foundation of China (Grant Nos. 11504106, 11805065, 11247308, and 11447167) and the Fundamental Research Funds for the Central Universities, China (Grant Nos. 2018MS049 and 2018MS056).

†Corresponding author. E-mail: slchern@ncepu.edu.cn

© 2018 Chinese Physical Society and IOP Publishing Ltd

the spin-1/2 states are given by the Pauli matrices, $S_j^{x,y,z} = \hbar\sigma^{x,y,z}/2$. In the following discussion, we set the Heisenberg coupling constants and the DM interaction to be dimensionless. The Planck constant $\hbar$ is set to be 1. Under the basis, $\{|\uparrow\uparrow\rangle, |\uparrow\downarrow\rangle, |\downarrow\uparrow\rangle, |\downarrow\downarrow\rangle\}$, the finite temperature density matrix with the z-component parameter of the DM interaction can be written as a 4×4 matrix,

$$\rho_1 = \frac{1}{Z_1}\begin{pmatrix} \rho_1^{11} & 0 & 0 & 0 \\ 0 & \rho_1^{22} & \rho_1^{23} & 0 \\ 0 & \rho_1^{23*} & \rho_1^{22} & 0 \\ 0 & 0 & 0 & \rho_1^{11} \end{pmatrix}, \tag{2}$$

where k is the Boltzmann constant and T is the temperature. $\rho_1^{23} = -\alpha_1 \mathrm{e}^{\theta_1}\sinh(\Sigma_1)/\Delta_1$, $\rho_1^{22} = \mathrm{e}^{\theta_1}\cosh(\Sigma_1)$, $\rho_1^{11} = \mathrm{e}^{-\theta_1}$, $\theta_1 = J_z/4kT$, $\Sigma_1 = \Delta_1/2kT$, $\alpha_1 = J + \mathrm{i}D_z$, $\Delta_1 = \sqrt{J^2 + D_z^2}$. Z_1 in the denominator is the partition function, whose expression is given by

$$Z_1 = \mathrm{Tr}(\mathrm{e}^{-H_1/kT}) = 2\mathrm{e}^{-\theta_1} + \mathrm{e}^{\theta_1}\cosh(\Sigma_1). \tag{3}$$

The second Hamiltonian is the XXZ Heisenberg model with an x-component DM interaction, which can be expressed as

$$H_2 = J\left(S_1^x S_2^x + S_1^y S_2^y\right) + J_z S_1^z S_2^z + D_x(S_1^y S_2^z - S_1^z S_2^y), \tag{4}$$

where D_x is the x component of the DM interaction. The 4×4 finite temperature density matrix can be expressed as follows:

$$\rho_2 = \frac{1}{Z_2}\begin{pmatrix} \rho_2^{11} & -\rho_2^{12} & \rho_2^{12} & \rho_2^{14} \\ \rho_2^{12} & \rho_2^{22} & \rho_2^{23} & -\rho_2^{12} \\ -\rho_2^{12} & \rho_2^{23} & \rho_2^{22} & \rho_2^{12} \\ \rho_2^{14} & \rho_2^{12} & -\rho_2^{12} & \rho_2^{11} \end{pmatrix}, \tag{5}$$

where $\rho_2^{11} = \mathrm{e}^{-\theta_1}/2 + 4\mathrm{e}^{\nu_1}D_x^2(\mathrm{e}^{-\lambda_1}/\omega_1 + \mathrm{e}^{\lambda_1}/\Gamma_1)$, $\rho_2^{12} = -\mathrm{i}\,\mathrm{e}^{\nu_1}D_x\sinh(\lambda_1)/\eta_1$, $\rho_2^{14} = \mathrm{e}^{-\theta_1}/2 - 4\mathrm{e}^{\nu_1}D_x^2(\mathrm{e}^{-\lambda_1}/\omega_1 + \mathrm{e}^{\lambda_1}/\Gamma_1)$, $\rho_2^{22} = \mathrm{e}^{-\Omega_1}/2 + \mathrm{e}^{\nu_1}(\alpha_2\mathrm{e}^{\lambda_1} - \beta_2\mathrm{e}^{-\lambda_1})/4\eta_1$, $\rho_2^{23} = \mathrm{e}^{-\Omega_1}/2 + \mathrm{e}^{\nu_1}(\beta_2\mathrm{e}^{-\lambda_1} - \alpha_2\mathrm{e}^{\lambda_1})/4\eta_1$, $\nu_1 = J/4kT$, $\lambda_1 = \eta_1/4kT$, $\Omega_1 = \Sigma_2/4kT$, $\Sigma_2 = 2J - J_z$, $\Gamma_1 = 8D_x^2 + 2\alpha_2^2$, $\omega_1 = 8D_x^2 + 2\beta_2^2$, $\alpha_2 = \Delta_2 + \eta_1$, $\beta_2 = \Delta_2 - \eta_1$, $\eta_1 = \sqrt{4D_x^2 + \Delta_2^2}$, $\Delta_2 = J + J_z$. The finite temperature partition function of this model Hamiltonian is given by

$$\begin{aligned} Z_2 &= \mathrm{Tr}(\mathrm{e}^{-H_2/kT}) \\ &= \left\{\mathrm{e}^{-\theta_1} + \mathrm{e}^{-\Omega_1} + \mathrm{e}^{\lambda_1+\nu_1}\left(\frac{8D_x^2}{\Gamma_1} + \frac{\alpha_2}{2\eta_1}\right)\right. \\ &\quad \left. + \mathrm{e}^{-\lambda_1+\nu_1}\left(\frac{8D_x^2}{\omega_1} - \frac{\beta_2}{2\eta_1}\right)\right\}. \end{aligned} \tag{6}$$

The third Hamiltonian is the general Heisenberg model with both an external magnetic field and a z-component DM interaction,

$$H_3 = \sum_{i=x,y,z} J_i S_1^i S_2^i + B(S_1^z + S_2^z) + D_z(S_1^x S_2^y - S_1^y S_2^x), \tag{7}$$

where B represents the external magnetic field. The 4×4 finite temperature density matrix is

$$\rho_3 = \frac{1}{Z_3}\begin{pmatrix} \rho_3^{11} & 0 & 0 & \rho_3^{14} \\ 0 & \rho_3^{22} & \rho_3^{23} & 0 \\ 0 & \rho_3^{23*} & \rho_3^{22} & 0 \\ \rho_3^{14} & 0 & 0 & \rho_3^{44} \end{pmatrix}, \tag{8}$$

where $\rho_3^{11} = J_z/4 + B$, $\rho_3^{14} = (J_x - J_y)/4$, $\rho_3^{22} = -J_z/4$, $\rho_3^{23} = (J_x + J_y)/4 + \mathrm{i}D_z/2$, $\rho_3^{44} = J_z/4 - B$, $\Delta_3 = J_x - J_y$, $\Sigma_3 = J_x + J_y$, $\eta_2 = \sqrt{16B^2 + \Delta_3^2}$, $\Gamma_2 = \sqrt{4D_z^2 + \Sigma_3^2}$, $\alpha_3 = J_z/4kT$, $\beta_3 = \eta_2/4kT$, $\theta_2 = \Gamma_2/4kT$. The partition function,

$$Z_3 = \mathrm{Tr}(\mathrm{e}^{-H_3/kT}) = 2\mathrm{e}^{-\alpha_3}\cosh(\beta_3) + e^{\alpha_3}\cosh(\alpha_2). \tag{9}$$

Generally, equation (1) can be considered as a special case of Eq. (7) by setting $J_x = J_y = J$ and $B = 0$.

3. Quantum correlation measurements

Quantum steering,[11] dating back to Schrödinger in 1935, can be described by a collection of ensembles of distant quantum states based on Bob and Alice. Such systems in a two-spin state can be entitled assemblages. The assemblage,[32] $\{Q_{a|x}\}_{a,x}$, is related to Alice getting an output a when putting in x. For any no-signaling assemblage, it is satisfied with $p(a|x) = \mathrm{Tr}(\sigma_{a|x})$. These are strictly no-signaling condition in the quantum assemblages:

$$\sum_a Q_{a|x} = \sum_a Q_{a|x'}, \quad \forall x, x', \tag{10}$$

and the normalization condition,

$$\mathrm{Tr}\sum_a Q_{a|x} = 1, \quad \forall x. \tag{11}$$

Although a local hidden state model cannot produce the assemblages, it can be observed in two distant parties. We restrict ourselves in this work to a more detailed assemblage form,

$$\{Q_{a|x}\} = \sum_\lambda D_A(\lambda) Q_{a|x}(a,x,\lambda)\xi(\lambda), \quad \forall x, a, \tag{12}$$

where λ sent to Alice through assemblages is named a local hidden variable. $\xi(\lambda)$ is the normalized state. An assemblage $\{Q_{a|x}\}$ is unsteerable if there is a probability distribution $D_A(\lambda)$. Any assemblage that does not admit a local hidden state model as in Eq. (12) is called steerable. The assemblages can be divided into two parts, $\{Q_{a|x}^{\mathrm{S}}\}$ and $\{Q_{a|x}^{\mathrm{US}}\}$, where $\{Q_{a|x}^{\mathrm{S}}\}$ refers to the steerable part and the other part $\{Q_{a|x}^{\mathrm{US}}\}$ is unsteerable. The steerable weight (SW) is defined as the minimal value of $1-\chi$ with χ defined as a proper division of $Q_{a|x}$,

$$Q_{a|x} = \chi Q_{a|x}^{\mathrm{US}} + (1-\chi)Q_{a|x}^{\mathrm{S}}, \quad \forall a, x, \quad 0 \le \chi \le 1, \tag{13}$$

Obviously, the SW takes a value between 0 and 1. SW = 1 means the state is completely steerable, while $SW = 0$ means the state is completely unsteerable.

In order to get a complete understanding of the quantum correlation and quantum steering, we study three other measurements of quantum correlation, *i.e.*, the concurrence,[2] quantum discord,[3–6] and the robustness of coherence.[7] Now let us introduce the definitions of these measurements. The concurrence,[2] which is used to describe the quantum entanglement between two parts, is defined as follows for the two-qubit states:

$$\mathscr{C}(\rho) = \max\left\{0, \sqrt{\Lambda_1} - \sqrt{\Lambda_2} - \sqrt{\Lambda_3} - \sqrt{\Lambda_4}\right\}, \tag{14}$$

where Λ_1, Λ_2, Λ_3, and Λ_4 are the four eigenvalues of the following matrix in decreasing order,

$$\rho(\sigma_y \otimes \sigma_y)\rho^*(\sigma_y \otimes \sigma_y), \tag{15}$$

where ρ^* is the complex conjugate of the density matrix ρ.

The definition of quantum discord[3–6] for a bipartite state ρ^{AB} contains two different definitions of quantum mutual information which are extensions of two equivalent definitions of classical mutual information. Quantum mutual information,

$$\rho_{\mathrm{I}}^{\mathscr{A}\mathscr{B}} = S(\rho^{\mathscr{A}}) - S(\mathscr{A}|\mathscr{B}), \tag{16}$$

which is the total of corrections in the bipartite state, where $S(\mathscr{A}|\mathscr{B}) = S(\rho^{\mathscr{A}\mathscr{B}}) - S(\rho^{\mathscr{B}})$ is the conditional entropy of the $\mathscr{A}$ side. Alternative mutual information based on a general measurement $N^{\mathscr{B}}$ on party $\mathscr{B}$ can be written as

$$\rho_{N^{\mathscr{B}}}^{\mathscr{A}\mathscr{B}} = S(\rho^{\mathscr{A}}) - \sum_m p(m) S(\rho_m^{\mathscr{A}}) = S(\rho^{\mathscr{A}}) - S(\mathscr{A}|\mathscr{B}_C), \tag{17}$$

where $\rho_m^{\mathscr{A}}$ corresponds to $\mathscr{A}$'s state conditioned on $\mathscr{B}$'s measurement output m, and $S(\mathscr{A}|\mathscr{B}_C) = \sum_m p(m) S(\rho_m^{\mathscr{A}})$ is $\mathscr{A}$'s averaged entropy on the condition of $\mathscr{B}$'s measurement outcomes. $\rho_{\mathrm{I}}^{\mathscr{A}\mathscr{B}}$ is the classical correlation between $\mathscr{A}$ and $\mathscr{B}$. Obviously, we obtain a quantum correlation measurement

$$\rho_{\mathrm{I}}^{\mathscr{A}\mathscr{B}} - \rho_{N^{\mathscr{B}}}^{\mathscr{A}\mathscr{B}} = S(\mathscr{A}|\mathscr{B}_C) - S(\mathscr{A}|\mathscr{B}). \tag{18}$$

We can see

$$\mathscr{D}(\rho) = \min_{N^{\mathscr{B}}}(\rho_I^{\mathscr{A}\mathscr{B}} - \rho_{N^{\mathscr{B}}}^{\mathscr{A}\mathscr{B}}) = \min_{N^B}[S(\mathscr{A}|\mathscr{B}_C) - S(\mathscr{A}|\mathscr{B})]. \tag{19}$$

The last quantity we used to identify the quantum correlation is the robustness of coherence.[7] It is defined as follows. Let $\mathscr{D}(\mathbb{C}^d)$ be the convex set of density matrices acting on a d-dimensional Hilbert space and $\mathscr{I} \in \mathscr{D}(\mathbb{C}^d)$ be the incoherent states subset. Then the robustness of coherence is given by

$$\mathscr{C}_{\mathrm{R}}(\rho) = \min_{\tau \in \mathscr{D}(\mathbb{C}^d)} \left\{ s \geq 0 \middle| \frac{\rho + s\tau}{1+s} \in \mathscr{I} \right\}. \tag{20}$$

In previous studies,[29] the XXZ model with the DM interaction has been concentrated on the concurrence. In this paper, we take advantage of quantum steering to describe this model.

4. Results

Previous studies[29,30] show that the quantum entanglement between the two spins can be effectively enhanced by the DM interactions. Here we show that the SW can also be enhanced by the DM interactions. Figure 1 shows the SW *versus* temperature for different parameters. Figures 1(a) and 1(b) present the results for the XXZ model with the z-component DM interaction given in Eq. (1) and the XXZ model with the x-component DM interaction given in Eq. (4), respectively. One can find that the critical temperature where the SW vanishes increases with DM interactions. For a given temperature being lower than the critical temperature, the value of the SW is larger for a larger DM interaction.

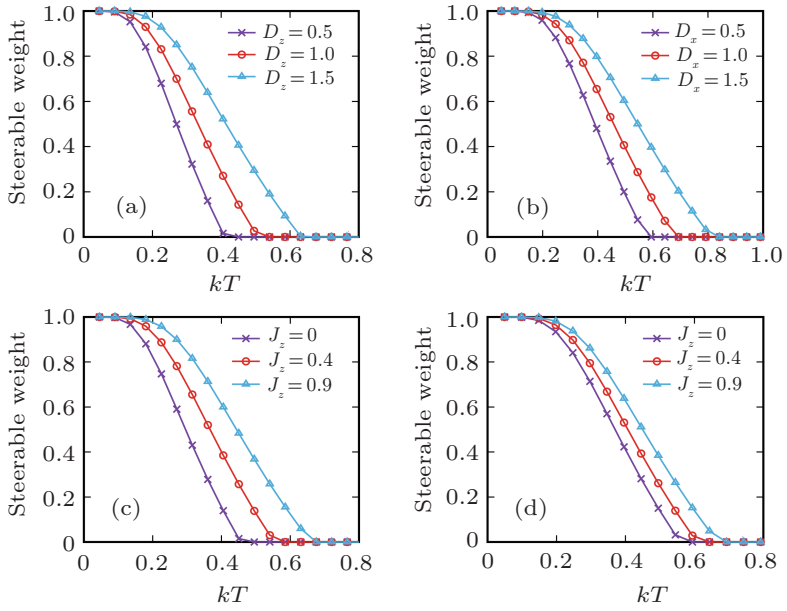


Fig. 1. (color online) The SW *versus* kT for different cases: (a) and (c), the XXZ model with z-component DM interaction shown in Eq. (1); (b) and (d), the XXZ model with x-component DM interaction shown in Eq. (4). $J = 1.0$ and $J_z = 0.2$ are chosen for plotting panels (a) and (b). $\{J, D_z\} = \{1.0, 1.0\}$ and $\{J, D_x\} = \{1.0, 1.0\}$ are chosen for plotting panels (c) and (d), respectively.

In Figs. 1(c) and 1(d), we show the SW *versus* temperature for different J_zs, where figure 1(c) gives the results for the XXZ model with the z-component DM interaction, and figure 1(d) presents the results for the XXZ model with the x-component DM interaction. For both of these two cases, one can find that the SW is enhanced by the anisotropic coupling J_z, *i.e.*, both the values of the SW and the critical temperature where the SW vanishes increase with J_z. In addition, by comparing the purple lines labeled with '$\times$' in figures 1(c) and 1(d), where $J = 1.0$, $J_z = 0$ are fixed and $D_z = D_x = 1.0$, we can find that the x component of the DM term is more efficient than the z component term in enhancing the SW. On the other hand, the blue lines labeled with '$\triangle$' are very close to each other, which demonstrates that, in this case ($J_z = 0.9$), the SW is dominated by the anisotropic term J_z rather than the DM term.

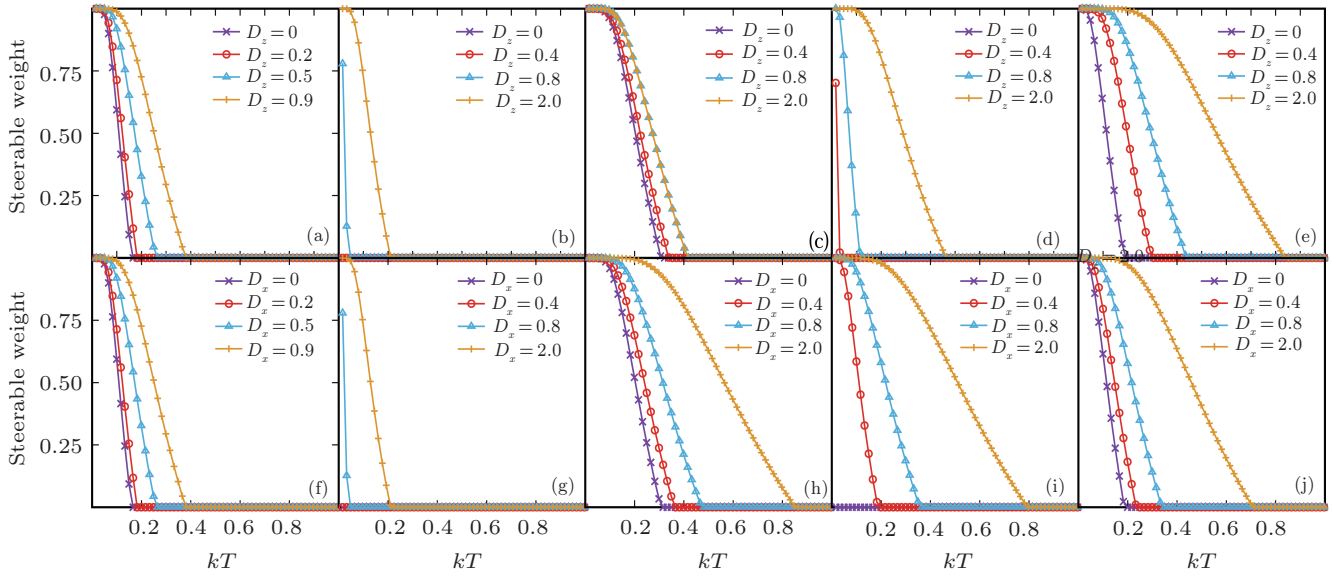


Fig. 2. (color online) The SW as a function of the absolute temperature kT for XXX model and XXZ model with different D_zs: (a) $J = J_z = 0.3$; (b) $J = J_z = -3.0$; (c) $J = 0.8$ and $J_z = 0.2$; (d) $J = 0.8$, $J_z = -0.8$; (e) $J = 0.2$ and $J_z = 0.8$. (f)–(j) The counter plots with the D_z term replaced by the D_x term.

Figures 2(a)–2(e) and figures 2(f)–2(j) show the SW as a function of kT for the different D_zs and D_xs presented in models Eq. (1) and Eq. (4), respectively. Here we focus on the effect of DM interactions in antiferromagnetic ($J > 0$) and ferromagnetic ($J < 0$) coupled systems. Figures 2(a) and 2(b) show the results for different D_zs in antiferromagnetically ($J = 0.3$) and ferromagnetically ($J = -3.0$) coupled XXX models. Figures 2(c) and 2(d) show the results for different D_zs in antiferromagnetically ($J = 0.8$, $J_z = 0.2$) and ferromagnetically ($J = 0.8$, $J_z = -0.8$) coupled XXZ models. For the ferromagnetically coupled states, as shown by the purple lines in Figs. 2(b) and 2(d), the SW vanishes for an arbitrary temperature. This is because the ground states are degenerated. Detailed calculations show that the density matrix of the ferromagnetically coupled XXX model at zero temperature is given by

$$\rho = \frac{1}{3}(|\uparrow\uparrow\rangle\langle\uparrow\uparrow| + |\downarrow\downarrow\rangle\langle\downarrow\downarrow| + \frac{1}{2}|\uparrow\downarrow + \downarrow\uparrow\rangle\langle\uparrow\downarrow + \downarrow\uparrow|).$$

Similarly, the ground state of the ferromagnetically coupled XXZ model presented in Fig. 2(d) is threefold degenerated,

$$\rho = \frac{1}{3}(|\downarrow\downarrow\rangle\langle\downarrow\downarrow| + \frac{1}{2}|\downarrow\uparrow - \uparrow\downarrow\rangle\langle\downarrow\uparrow - \uparrow\downarrow| + \frac{1}{2}|\uparrow\uparrow + \downarrow\downarrow\rangle\langle\uparrow\uparrow + \downarrow\downarrow|).$$

When $D_z \neq 0$, as shown in Figs. 2(b) and 2(d), the SW will have a finite value at zero temperature. The reason for this result is that the degeneracy of the ground state is lifted. On the other hand, as shown in Figs. 2(a) and 2(c), if the two qubits are antiferromagnetically coupled, the ground state will be the Bell state,

$$\rho = \frac{1}{2}|\uparrow\downarrow - \downarrow\uparrow\rangle\langle\uparrow\downarrow - \downarrow\uparrow|,$$

and the SW is not vanishing. In addition, the purple lines labeled with '$\times$' in Figs. 2(a) and 2(c) are very close to the red lines labeled with '$\circ$', which demonstrates that, in this case (D_z is relatively small), the SW is dominated by thermal fluctuations. Next, we compare the effects of the z component and x component of the DM interaction on the SW. For the isotropic XXX model shown in Figs. 2(a), 2(f) (antiferromagnetic), and Figs. 2(b), 2(g) (ferromagnetic), we find that the SW is independent of the orientation of the DM interaction. This is induced by the spin rotation symmetry of the XXX model. When $J > J_z$, we find that, as shown in Figs. 2(c), 2(d), and 2(h), 2(i), the D_x is more efficient in enhancing the SW. However, when $J < J_z$, the D_z is more efficient (see Figs. 2(e) and 2(j) for details). This is ascribed to the purity of the density matrix. It is easy to check that the energy gap between the first excited state and the ground state is smaller for the D_z

case if $J > J_z$. This smaller energy gap makes the purity of the density matrix lower at finite temperature, so that the SW is more easily destroyed by thermal fluctuation. When $J < J_z$, it is the opposite.

Now we study the Ising model with a transverse magnetic field, which is a special case of the model Hamiltonian Eq. (7) by taking $J_y = J_z = 0$.

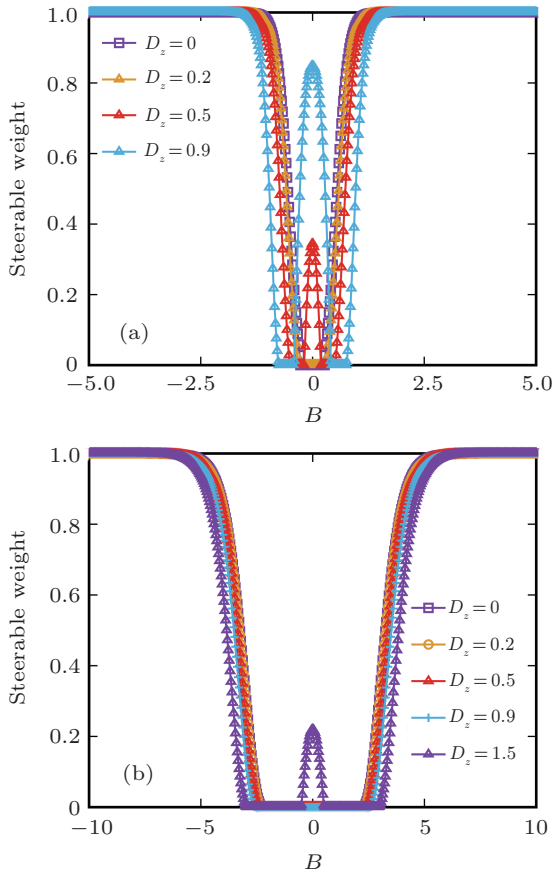


Fig. 3. (color online) The SW is plotted as a function of the external magnetic field B for different D_z in $kT = 0.1$ (a) with $J_x = 0.8$, $J_y = J_z = 0$; and in $kT = 0.4$ (b) with $J_x = 0.8$, $J_y = J_z = 0$.

Figures 3(a) and 3(b) show the SW *versus* the external magnetic field B for fixed temperatures $kT = 0.1$ and $kT = 0.4$, respectively. Generally, in the strong magnetic field limit, $|B| \to \infty$, SW $\to 1$, for different DM interactions. For the special case with $D_z = 0$ (the purple lines labeled with '□'), the results are consistent with those given in Ref. [33]. Comparing Figs. 3(a) and 3(b), one can find that there is an additional in-gap peak near $B = 0$ in Fig. 3(a) for the red line and blue line labeled with '△' and '▲', respectively. The disappearing when $D_z < 1$ of these in-gap peaks in Fig. 3(b) is easy to understand. In the high-temperature regime, the SW is suppressed by thermal fluctuation. Only when $D_z > 1.2$ is big enough to overcome the thermal fluctuations, there is an additional in-gap peak near $B = 0$ in Fig. 3(b). For the special case with $D_z = 0$, *i.e.*, the purple line labeled with '□', the in-gap peak disappears. This is induced by ground state degeneracy. Straightforward calculations show that the ground state for the model Hamiltonian Eq. (7) with $D_z = B = J_y = J_z = 0$ is twofold degenerated,

$$\rho = \frac{1}{4}(|\downarrow\downarrow - \uparrow\uparrow\rangle\langle\downarrow\downarrow - \uparrow\uparrow| + |\downarrow\uparrow - \uparrow\downarrow\rangle\langle\downarrow\uparrow - \uparrow\downarrow|).$$

This result demonstrates that the in-gap peak in Fig. 3(a) is induced by the DM interaction. After some tedious but straightforward calculations, we find that the ground state degeneracy is lifted by the DM interaction. The eigenvalue of the ground state is $-\sqrt{4+25D_z^2}/10$ and the corresponding (unnormalized) eigenvector is $(0, -\mathrm{i}\sqrt{4+25D_z^2}, 2\mathrm{i}+5D_z, 0)$. The eigenvalue of the first excited state is $-1/5$. The energy gap between the ground state and the first excited state increases with D_z, such that the SW is more robust against thermal fluctuation for larger D_z. This explains why the in-gap peak is higher for a larger D_z.

In order to get a more intuitive understanding of the quantum correlation and quantum steering of the model Hamiltonian Eq. (7) affected by the DM interaction, here we study the other measurements, *i.e.*, the concurrence, quantum discord, and the robustness of coherence. The numerical results are shown in Figs. 4(a)–4(c), and the temperature is chosen to be $kT = 0.4$ in the numerical calculations.

Figure 4(a) presents the concurrence of the Ising model with respect to the external magnetic field B for different DM interactions. As shown by the purple lines in the plotting, the quantum concurrence is zero when $D_z = 0$ and $B = 0$. When D_z increases to a finite value, *i.e.*, $D_z = 0.7$, there is an in-gap peak near $B = 0$. Previous studies[34] demonstrated that the DM interaction can delay the quantum phase transition, where the concurrence suddenly drops to zero at a finite magnetic field in the regime $0 < |B| < 5$, *i.e.*, the critical value $|B_c| \approx 2$ for $D_z = 1.5$ as shown by the red line labeled with '+' in the figure. In addition, previous investigation[35] showed that the concurrence has a maximum at a low temperature and with a weak magnetic field applied. As we can see, there is an additional peak in the regime $0 < |B| < 5$. Generally, the DM interaction and the external magnetic field play competing roles in enhancing the quantum concurrence. In the strong magnetic field regime, as demonstrated in Ref. [35], the field influence on the concurrence behavior will overcome the DM interaction, such that the concurrence drops again and all the lines shown in Fig. 4(a) tend to overlap.

Figure 4(b) presents the quantum discord of the Ising model as a function of the external magnetic field for different DM interactions at $kT = 0.4$. It is not hard to see that $\mathscr{D}(\rho) = 0$ for the special case at $B = 0$ and $D_z = 0$. Meanwhile, for the fixed value $B = 0$, the stronger the DM interaction, the larger the value of the quantum discord. These results coincide with those given in Ref. [30]. As shown by the purple, green, and blue lines for $D_z = 0$, 0.5, and 0.9, there are bimodal structures due to the fact that the discord in fixed temperature will reach

a maximal value when the magnetic field and DM interaction are roughly equal to each other. For a very large DM interaction, *i.e.*, $D_z = 1.5$, our calculation shows that the bimodal structure disappears and $\mathscr{D}(\rho)$ gets a large value at $B = 0$.

As shown in Fig. 4(a), there are zero points near $|B| = 1$; however, the discord shown in Fig. 4(b) exhibits a bimodal structure in this regime for small D_zs. Here we give an intuitive explanation. When both B and D_z are vanishing, the ground states are the twofold-degenerated product states, so one can find that, in this case, both concurrence and discord are zero. Detailed calculations show that, as D_z increases ($B = 0$ fixed), the degenerated states are lifted, and the ground state prefers the antiferromagnetic-like entangled state, $(-J_x - 2iD_z)/\sqrt{J_x^2 + 4D_z^2}|\uparrow\downarrow\rangle + |\downarrow\uparrow\rangle$. On the other hand, if we make $D_z = 0$ fixed and $|B|$ increasing, the ground state reveals the ferromagnetic-like entangled state, $|\uparrow\uparrow\rangle + J_x/\left(4B - \sqrt{16B^2 + J_x^2}\right)|\downarrow\downarrow\rangle$. There is a quantum phase transition between these two states. The transition point is located at $2|B| = D_z$. At this phase transition point, these two states blend and the quantum entanglement vanishes. This explains not only the zero points near $|B| = 1$ in Fig. 4(a), but also the zero points in Fig. 3 in the same regimes. Due to the fact that these two states are both entangled, the quantum correlation does not vanish.

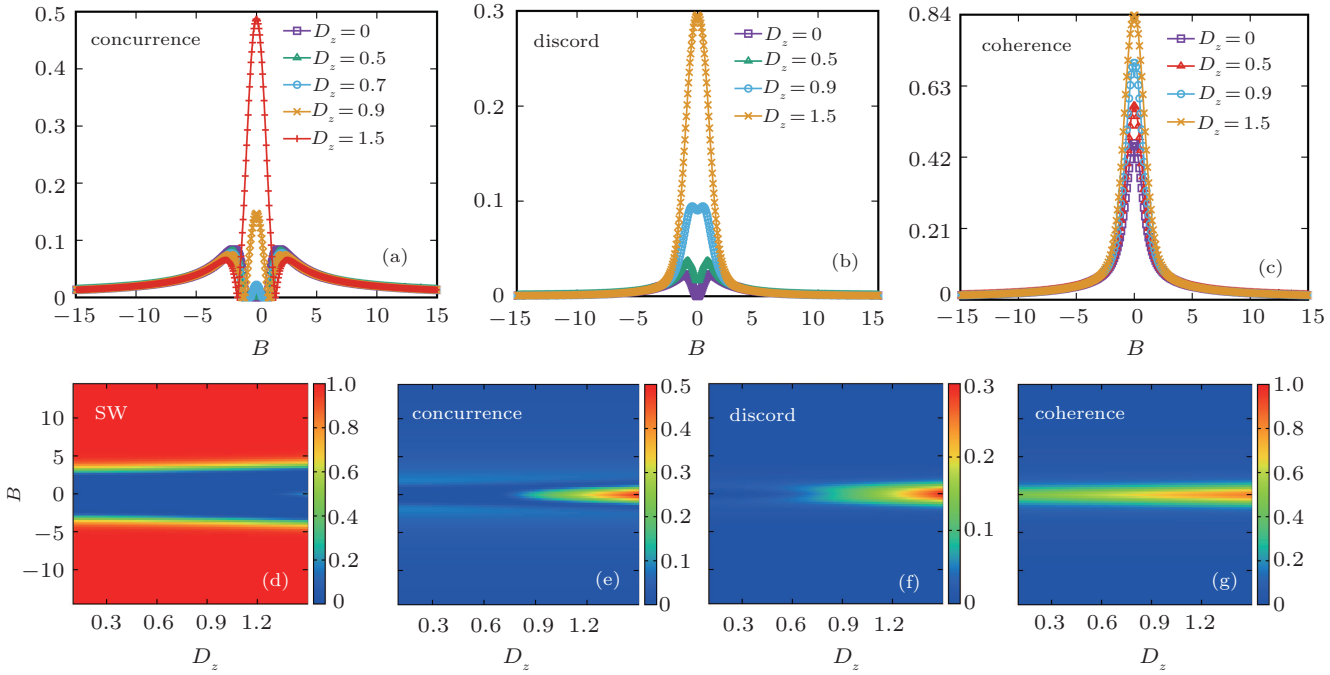


Fig. 4. (color online) (a)–(c) The concurrence, quantum discord, and robustness of coherence as functions of the external magnetic field B for the Ising model, $J_y = J_z = 0$, $J_x = 0.8$, and different D_zs. (d)–(g) The contour plots of the SW, quantum concurrence, quantum discord, and quantum coherence as functions of D_z ranging from 0 to 1.5 and magnetic field B from -15 to 15. $kT = 0.4$ is set in all the plots.

In Fig. 4(c), we conduct a quantitative study of quantum coherence. Numerical calculations show that, for the Heisenberg model with the DM interaction, the robustness of coherence equals the norm-1 coherence, which is defined as the summation of the absolute value of the off-diagonal elements of the density matrix. Taking the summation over all the off-diagonal elements of the density matrix given in Eq. (8), we can obtain an analytic expression of the robustness of coherence,

$$\mathscr{C}_R(\rho) = 2\mathrm{e}^{-\alpha_3}\frac{\Delta_3}{\sqrt{16B^2+\Delta_3^2}}\sinh\left(\frac{\sqrt{16B^2+\Delta_3^2}}{4kT}\right) - 2\mathrm{e}^{\alpha_3}\frac{\Sigma_3}{\sqrt{4D_z^2+\Sigma_3^2}}\sinh\left(\frac{\sqrt{4D_z^2+\Sigma_3^2}}{4kT}\right).$$

After some tedious but straightforward calculations, we find that $\mathscr{C}_R(\rho)$ takes the maximum at $B = 0$. From the analytic expression, we can find that the coherence is negative-proportional to the transverse magnetic field $|B|$, which is demonstrated in the plotting. At the fixed point $B = 0$, we find that $\mathscr{C}_R(\rho)$ is positively correlated to the DM interaction. In addition, in the strong magnetic field limit, $|B| \to \infty$, the influence of D_z is negligible, and the four lines tend to completely overlap.

Figures 4(d)–4(g) show the contour plots of the four measurements, SW, quantum concurrence, quantum discord, and quantum coherence *versus* the DM interaction and magnetic field. Figure 4(d) shows that the SW enhances with D_z and the external magnetic field, respectively. For the special case $B = 0$, SW$\to 1$ for a large DM interaction, *i.e.*, $D_z = 1.2$. This result coincides with the additional in-gap peak shown in Fig. 3(b). When the external magnetic field is big enough, *i.e.*, $|B| \geq 5$, it is almost maximally steerable. Figure 4(e) gives a panoramic view of the concurrence for different D_z and

B. Here we find that the concurrence increases when D_z increases, while the influence of B on the concurrence is different from the D_zs. The concurrence increases near the $B = 0$ point while it decreases beyond this region. The contour plot of quantum discord, as shown in Fig. 4(f), is similar to the concurrence. The only difference is that the quantum discord converges two peaks into a single peak with D_z increasing, which corresponds to the transformation from a bimodal structure to a single peak as D_z increases, as shown in Fig. 4(b). As shown in Fig. 4(g), we find that the coherence increases with the D_z while it decreases with the external magnetic field. These contour plots show clearly that: (i) the SW can be preserved in the strong magnetic field which is dramatically different from the other measurements, and (ii) the DM interaction plays a positive role in enhancing both the SW and other quantum correlations.

5. Summary

In this work, we study the influence of the DM interaction on the quantum entanglement of the two-qubit Heisenberg model, realizing the difference between the SW and other measurements, *i.e.*, the concurrence, the quantum discord, and the robustness of the coherence. We find that the DM interaction and the anisotropic coupling can effectively enhance the value of the SW. In addition, with the increase of J_z, D_x, and D_z, the critical temperature and the entanglement increase. Furthermore, the influence of D_x is more obvious than that of D_z for the XXZ model if $J > J_z$. If $J < J_z$, the influence of D_z is more obvious. Meanwhile, as the temperature rises, the SW will survive and behave robustly in the strong magnetic field regime when the thermal fluctuation of the system exceeds the quantum effect. Last but not least, the increase of the DM interaction, at a specific temperature (low temperature) or in a particular system (ferromagnetic), can lift the degeneracy of the ground state and make the SW go from zero to a finite value.

References

[1] Amico L, Fazio R, Osterloh A and Vedral V 2008 *Rev. Mod. Phys.* **80** 517
[2] Wootters W K 1998 *Phys. Rev. Lett.* **80** 2245
[3] Henderson L and Vedral V 2001 *J. Phys. A: Math. Gen.* **34** 6899
[4] Ollivier H and Zurek W H 2001 *Phys. Rev. Lett.* **88** 017901
[5] Ren X J and Fan H 2012 *J. Phys. A: Math. Theor.* **45** 425304
[6] Ollivier H and Zurek W H 2001 *Phys. Rev. Lett.* **88** 017901
[7] Napoli C, Bromley T R, Cianciaruso M, Piani M, Johnston N and Adesso G 2016 *Phys. Rev. Lett.* **116** 150502
[8] Schrödinger E 1935 *Math. Proc. Cambridge Philos. Soc.* **31** 555563
[9] Schrödinger E 1936 *Math. Proc. Cambridge Philos. Soc.* **32** 446452
[10] Einstein A, Podolsky B and Rosen N 1935 *Phys. Rev.* **47** 777
[11] Wiseman H M, Jones S J and Doherty A C 2007 *Phys. Rev. Lett.* **98** 140402
[12] Jones S J, Wiseman H M and Doherty A C 2007 *Phys. Rev. A* **76** 052116
[13] Skrzypczyk P, Navascués M and Cavalcanti D 2014 *Phys. Rev. Lett.* **112** 180404
[14] Bowles J, Vértesi T, Quintino M T and Brunner N 2014 *Phys. Rev. Lett.* **112** 200402
[15] He Q Y, Gong Q H and Reid M D 2015 *Phys. Rev. Lett.* **114** 060402
[16] Kogias I, Lee A R, Ragy S and Adesso G 2015 *Phys. Rev. Lett.* **114** 060403
[17] Bowles J, Francfort J, Fillettaz M, Hirsch F and Brunner N 2016 *Phys. Rev. Lett.* **116** 130401
[18] Bowles J, Hirsch F, Quintino M T and Brunner N 2016 *Phys. Rev. A* **93** 022121
[19] Sun W Y, Wang D, Shi J D and Ye L 2017 *Sci. Rep.* **7** 39651
[20] Saunders D J, Jones S J, Wiseman H M and Pryde G J 2010 *Nat. Phys.* **6** 845
[21] Kocsis S, Hall M J W, Bennet A J, Saunders D J and Pryde G J 2015 *Nat. Commun.* **6** 5886
[22] Sun K, Xu J S, Ye X J, Wu Y C, Chen J L, Li C F and Guo G C 2014 *Phys. Rev. Lett.* **113** 140402
[23] Sun K, Ye X J, Xu J S, Xu X Y, Tang J S, Wu Y C, Chen J L, Li C F and Guo G C 2016 *Phys. Rev. Lett.* **116** 160404
[24] Wollmann S, Walk N, Bennet A J, Wiseman H M and Pryde G J 2016 *Phys. Rev. Lett.* **116** 160403
[25] He Q, Rosales-Zárate L, Adesso G and Reid M D 2015 *Phys. Rev. Lett.* **115** 180502
[26] Branciard C, Cavalcanti E G, Walborn S P, Scarani V and Wiseman, H M 2012 *Phys. Rev. A* **85** 010301
[27] Paul T 2007 *Math. Struct. Comp. Sci.* **17** 1115
[28] Qian L and Fang J X 2009 *Commun. Theor. Phys.* **52** 817
[29] Li D C, Wang X P and Cao Z L 2008 *J. Phys.: Condens. Matter* **20** 325229
[30] Ma X S, Cheng M T, Zhao G X and Wang A M 2012 *Physica A* **391** 2500
[31] Werlang T and Rigolin G 2010 *Phys. Rev. A* **81** 044101
[32] Gallego R and Aolita L 2015 *Phys. Rev. X* **5** 041008
[33] Chen L and Zhang Y Q 2017 *Europhys. Lett.* **120** 60007
[34] Khan S and Khan K 2016 *Eur. Phys. J. Plus* **131** 1
[35] Zad H A and Movahhedian H 2017 *Int. J. Mod. Phys. B* **31** 1750094